Journal of Organometallic Chemistry 776 (2015) 98–106

Contents lists available at ScienceDirect

Journal of Organometallic Chemistry

journal homepage: www.elsevier.com/locate/jorganchem

Synthesis, characterization, photoluminescence and computational studies of mono- and diorgano-gallium complexes containing azo linked salicylaldimine Schiff bases

Manoj K. Pal [a], Nisha Kushwah [a], Amey P. Wadawale [a], Debashree Manna [b], V. Sudarsan [a], Tapan K. Ghanty [b], Vimal K. Jain [a, *]

[a] Chemistry Division, Bhabha Atomic Research Centre, Trombay, Mumbai 400 085, India
[b] Theoretical Chemistry Section, Bhabha Atomic Research Centre, Trombay, Mumbai 400 085, India

ARTICLE INFO

Article history:
Received 23 June 2014
Received in revised form
10 October 2014
Accepted 16 October 2014
Available online 6 November 2014

Keywords:
Organogallium
Phenylazo salicyldehyde
Schiff base
Photoluminescence
X-ray structure

ABSTRACT

The reactions of triorgano-gallium etherate with azo linked salicylaldimine Schiff bases in benzene gave complexes of the type $[R_2GaOC_6H_3(N{=}NPh)(CH{=}NAr)]$, $[R_2GaOC_6H_3(N{=}NPh)(CH{=}NCH_2{-})]_2$, $[\{R_2GaOC_6H_3(N{=}NPh)(CH{=}NCH_2CH_2\}_3N]$ and $[C_6H_5{-}N{=}N{-}C_6H_3(4'\text{-}OGaRO)\text{-}3'\text{-}CH{=}N{-}C_6H_4]$ (R = Me or Et; Ar = Ph or tol-4). These complexes have been characterized by elemental analysis, IR, UV–Vis, NMR (^1H and $^{13}C\{^1H\}$) spectroscopy. The molecular structures of $[Me_2GaOC_6H_3(N{=}NPh)CH{=}NPh]\cdot\frac{1}{2}C_6H_6$ (**5a**·½C_6H_6) and $[Me_2GaOC_6H_3(N{=}NPh)(CH{=}Ntol\text{-}4)]$ (**5c**) were established by X-ray crystallography. Density functional calculations have also been performed to obtain structure and energetic information for the bare ligands and the metal-ligand complexes. Photoluminescence studies of these complexes showed that the quantum yield is always higher than that of the corresponding ligands and the emission peaks of complexes are blue shifted with respect to ligand.

Introduction

There has been an enduring interest for quite some time in organogallium complexes derived from internally functionalized anionic oxo-ligands [1]. These complexes exhibit a wide structural diversity [1–3] and polymorphism [4]; find applications in catalysis [4,5], materials science [6,7] and biomedical imaging [8] and show interesting photo-physical properties [2–4,9].

Remarkable photo-physical properties of group 13 metal complexes, in particular tris(8-hydroxyquinolate)aluminum(III) (AlQ_3) [10], have been extensively exploited in organic light emitting diodes (OLEDs) display devices [11]. The low photo-luminescent quantum yield and electron mobility of AlQ_3 necessitated exploration of a wide range of luminescent group 13 metal complexes [11,12]. The higher power efficiency of GaQ_3 in light emitting devices than that of AlQ_3 [13] suggests that the gallium complexes may be better luminescent material for display applications. Accordingly gallium complexes, both classical [14–16] and organometallic [2–4,9,17], have been designed with reference to their photo-physical properties. Diorganogallium complexes with anionic bidentate ligands capable of forming six-membered chelate rings preferentially exist as four-coordinate monomeric species. The hydrolytic stability of these complexes varies with the nature of ligand, N-alkyl salicylaldimidate complexes being hydrolytically most stable [18]. The latter complexes are photo emissive in solution [2,4].

There are numerous photochromic anionic ligands, in particular compounds with azo chromophore (–N=N–) are of considerable interest. Besides their classical applications in synthetic azo dyes and pigments [19], pharmaceuticals [20], their use in photo-responsive biomaterials is emerging [21]. Photochromism of azobenzene chromophores on light irradiation is well documented [22,23]. The 5-phenylazo salicylidene imines represent an interesting family of photochromic molecules [24,25] and have been utilized to prepare metal complexes [26] and several of them exhibit photo-luminescence in solution. With this perspective we have synthesized a series of mono- and diorgano-gallium complexes derived from 5-phenylazo salicylidene imine ligands (**1**–**4**) and characterized them by spectroscopic methods, and studied their photo-physical properties. Results of this work are reported herein.

* Corresponding author. Tel.: +91 22 2559 5095; fax: +91 22 2550 5151.
E-mail address: jainvk@barc.gov.in (V.K. Jain).

http://dx.doi.org/10.1016/j.jorganchem.2014.10.024
0022-328X/

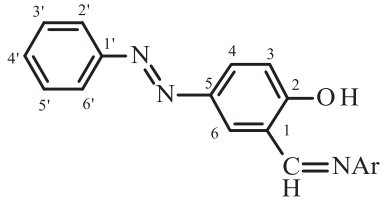

(1)

Ar = Ph (**1a**) or 4-MeC_6H_4 (**1b**)

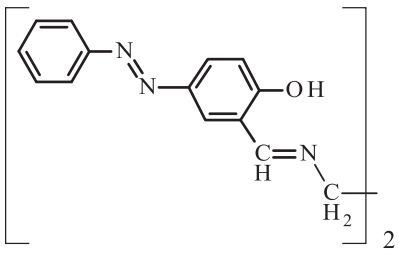

(2)

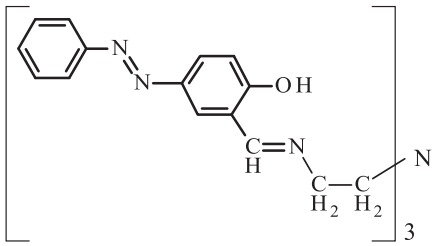

(3)

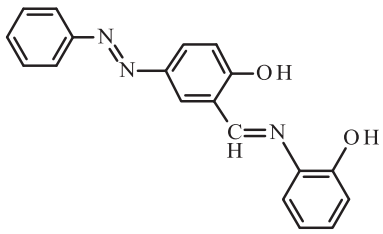

(4)

Results and discussion

Synthesis and characterization of complexes

Reactions of [5-(phenylazo)-N-(aniline)salicylidene] (**1a**), [5-(phenylazo)-N-(*p*-toluidine)salicylidene] (**1b**), bis(5-phenylazo salicyldehyde)ethylenediimine (**2**), tris{(5-phenylazo salicyldehyde) amino ethyl}amine (**3**) and [5-(phenylazo)-N-(2-hydroxyphenyl) salicylidene] (**4**), with trialkyl gallium etherate in benzene at room temperature afforded dialkyl or monoalkyl gallium complexes (Scheme 1) as yellow to orange-red solids or paste.

The IR spectra of these complexes displayed absorptions in the regions 557–591 and 515–536 cm^{-1}, which were absent in the corresponding free ligands. These absorptions have been assigned to Ga–C and Ga–O, respectively based on IR spectral data for similar compounds [2,4,27] and $[Me_2Ga(OH)]_4$ [28]. The absorption due to azomethine linkage (–CH=N–) are slightly shifted to lower wave numbers with respect to the free ligand on coordination of

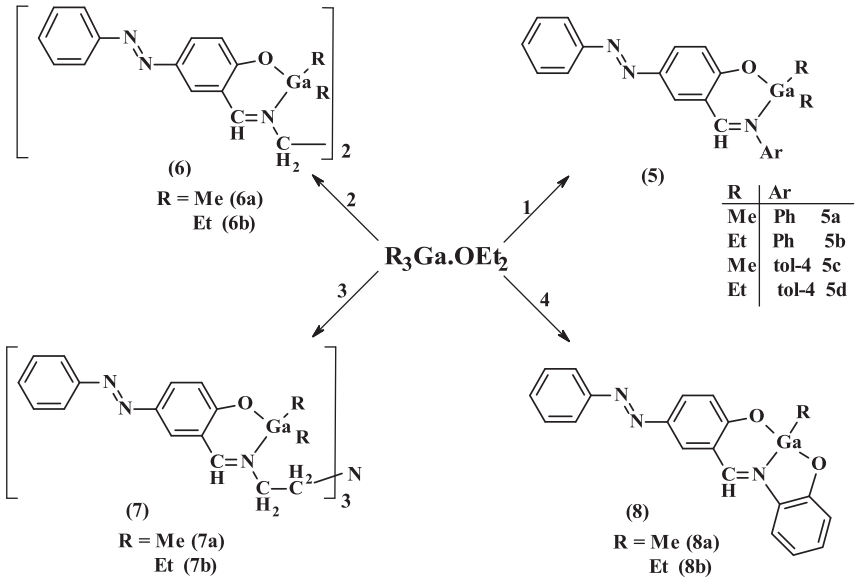

Scheme 1. Synthesis of organogallium complexes.

nitrogen atom to gallium. The stretchings due to azo functional group (N=N) are also shifted to lower wave numbers (13–23 cm^{-1}) on coordination with ligand (in gallium complexes 1468–1483 cm^{-1} and for free ligands 1487–1499 cm^{-1}).

The ^{1}H and ^{13}C NMR spectra, recorded in dmso-d_6, displayed characteristic peaks with expected multiplicities for metal alkyl and ligand fragment. The dimethylgallium complexes showed a characteristic high-field singlet due to methyl group at $\delta \sim -0.30$ and -5.3 to -6.2 ppm in the ^{1}H and ^{13}C NMR spectra, respectively. The methyl resonance for mono methylgallium complex (**8a**) is further shielded. The ^{13}C NMR resonances due to –CH=N– in diorgano gallium complexes is deshielded by 5.7–7.2 ppm from the respective resonance for the free ligand, while for mono-organo gallium complexes (**8a**, **8b**) the signal is shielded by 2.6 ppm from **4**. The proton resonances of –CH=N– group, however, showed a different pattern. The signal is shielded for complexes derived from **1a** and **1b**, while there is deshielding for complexes formed from **2** and **3**, whereas the resonance is little influenced for the complexes formed by **4**. The ^{13}C NMR resonances assignable to C-2, C-3 and C-4′ are deshielded with respect to the corresponding resonances for the free ligand.

Organogallium complexes derived from salicylidene based ligands are known to exist as discrete monomeric molecules [2,4,18]. The spectroscopic data for structurally characterized complexes (**5a** and **5c**, see later) are similar to the data for other complexes indicating that various complexes have formulation as shown in Scheme 1, which is further substantiated by analytical data.

*Crystal structures of **5a** and **5c***

The molecular structures of $[Me_2GaOC_6H_3(N{=}NPh)CH{=}NPh]\cdot\frac{1}{2}C_6H_6$ (**5a**·$\frac{1}{2}C_6H_6$) and $[Me_2GaOC_6H_3(N{=}NPh)CH{=}Ntol\text{-}4]$ (**5c**) were established by single crystal X-ray diffraction analyses. Perspective drawings are depicted in Figs. 1 and 2, while their selected interatomic parameters are given in Table 1. Both the complexes are discrete monomers with four coordinated gallium. The metal atom in each complex is coordinated to two methyl carbon atoms, phenolate oxygen and azomethine nitrogen forming a distorted tetrahedral structure. The six-membered O1–C3–C2–C2–N1–Ga1 chelate rings are almost but not completely planar with gallium atom and slightly above the mean plane (0.011 Å for **5a** and 0.162 Å for **5c**). The inter-planar angle between the O1–C3–C2–C2–N1–Ga1 mean plane and the C14–C15–C16–C17–C–18–C19 mean plane is 88.9° for **5a** and 76.7° **5c** (Figs. 1b and 2b). The phenylazo salicylidene fragment is slightly twisted along the N=N with a torsion angle 179.6 (4) and 179.6 (7)° in **5a** and **5c** respectively. The fragment O1–C3–C2–C2–N1 is coplanar with the adjoining phenyl ring of phenylazo salicylidene group. The Ga–C [4,29], Ga–O [4,6,30,31] and Ga–N [2,4,30,31] distances are in conformity with the values reported in the literature such as $[Me_2GaOC_6H_4CH{=}NCH_2{-}]_2$, $[MeGa\{-O(2\text{-}C_6H_4){-}CH{=}N(2\text{-}C_6H_4){-}O{-}\}]$ and $[Me_2Ga(\text{-}O_2C{-}C_5H_4N\text{-}2)]_2$, etc. In case of **5c** intra-molecular short contacts N2···H16–C16 (2.687 Å) between the azobenzene nitrogen and the phenyl salicylidene lead to the formation of weakly bonded dimers (Fig. 2c) whereas **5a** is devoid of any such interactions.

The electron releasing methyl group in the para position of aryl ring in the azomethine group is evident from Table 1. The azomethine linkage (C1–N1) is marginally shortened in tolyl substituted derivate (**5c**) than that of the phenyl substituted complex (**5a**). Consequently the Ga1–N1 bond is slightly elongated while the Ga1–O1 bond is shortened in the case of **5c** as compared to the corresponding values in **5a**. The C20–Ga1–N1 angle is marginally

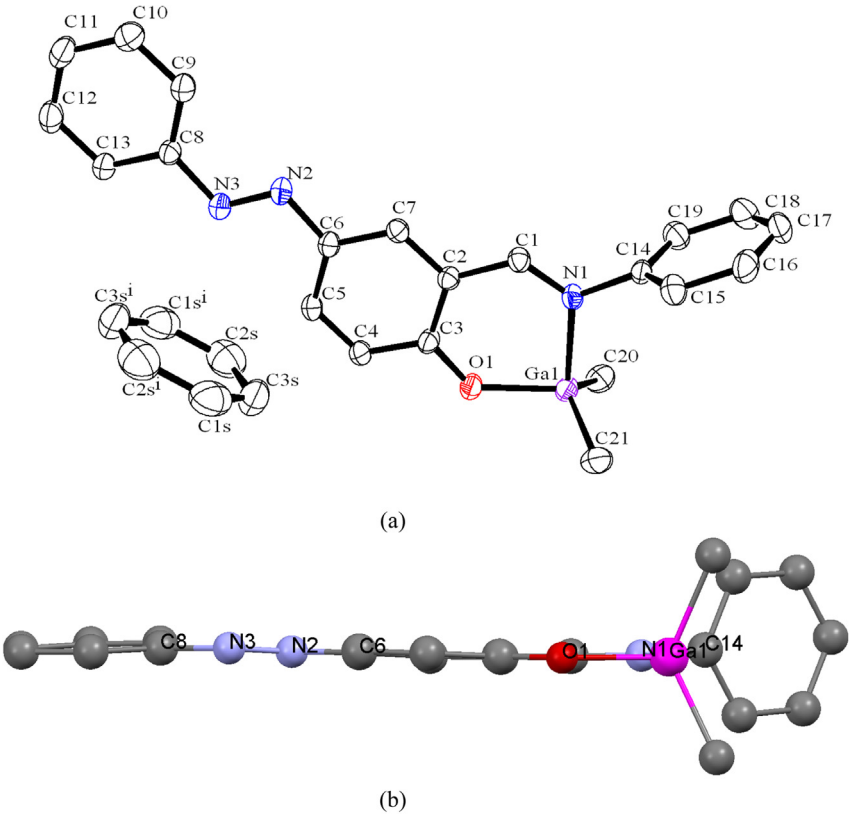

Fig. 1. (a) ORTEP drawing of $[Me_2GaOC_6H_3(N{=}NPh)(CH{=}NPh)]\cdot\frac{1}{2}C_6H_6$ (**5a**·$\frac{1}{2}C_6H_6$) with 25% thermal ellipsoid probability. Hydrogen atoms are omitted for clarity (b) Twist along the N=N in $[Me_2GaOC_6H_3(N{=}NPh)(CH{=}NPh)]\cdot\frac{1}{2}C_6H_6$ (**5a**·$\frac{1}{2}C_6H_6$) with torsion angle 179.6 (4)°.

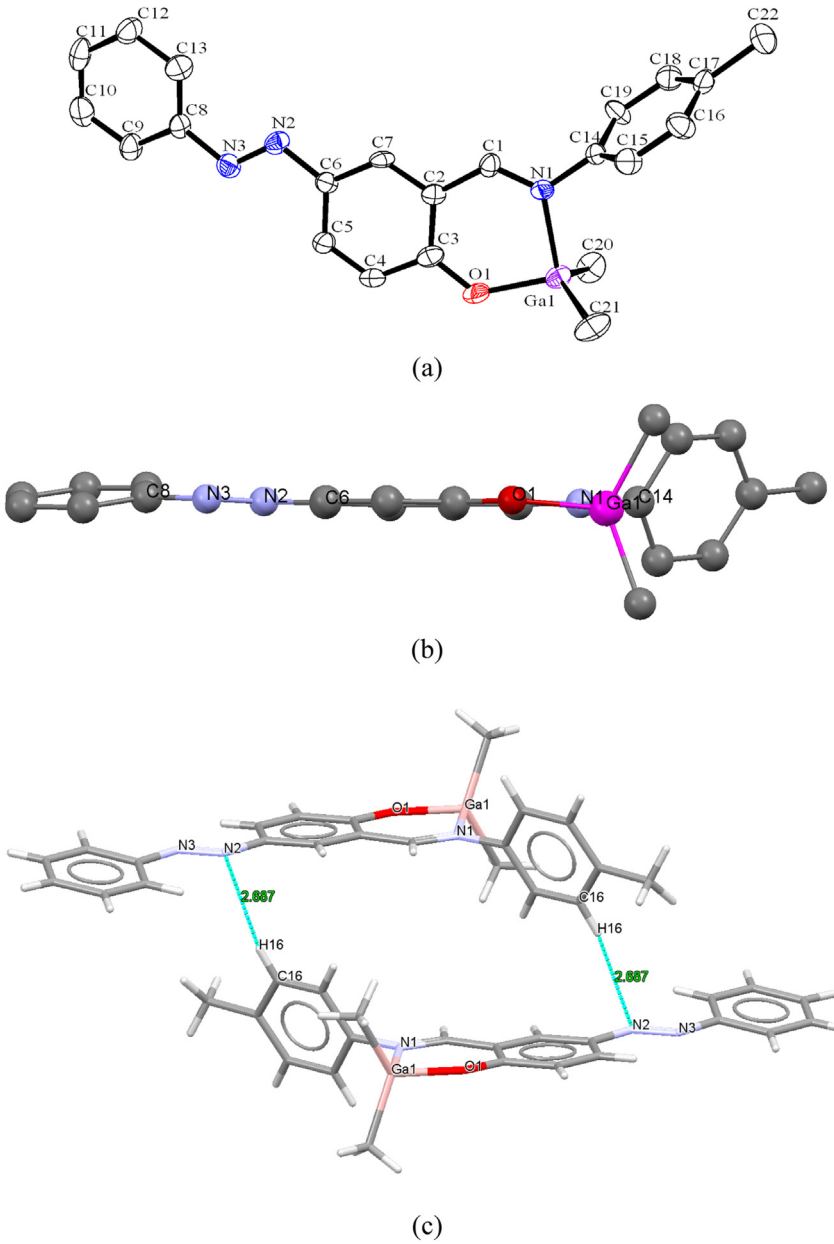

Fig. 2. (a) ORTEP drawing of [$Me_2GaOC_6H_3$(N═NPh) (CH═Ntol-4)] (**5c**) with 25% thermal ellipsoid probability. Hydrogen atoms are omitted for clarity; (b) Twist along the N═N in [$Me_2GaOC_6H_3$(N═NPh) (CH═Ntol-4)] (**5c**) with torsion angle 179.6 (7)°; (c) Dimers of [$Me_2GaOC_6H_3$(N═NPh) (CH═Ntol-4)] (**5c**) formed due to N–CH short interactions.

compressed in **5c** than **5a**, while converse is noted in C20–Ga1–C21 angle.

Photo-physical properties

Electronic absorption and emission spectra of the ligands and their organogallium complexes were recorded in dichloromethane and the resulting data are summarized in Table 2. The electronic spectra of free ligands displayed two broad peaks at ~275 nm and in the region 334–361 nm, the latter being more intense. The weak absorption at ~275 nm is attributed to π–π* transitions in the aromatic ring [26f]. Alternatively this can also arise from the *cis* form of the ligand [32]. Since the π–π* transitions of imine linkage and the azo group appear in a close proximity, the two may overlap in each other. Thus the broad absorption in the region 334–361 nm may be assigned to π–π* transitions in CH═N and N═N groups. The n–π* transitions for these groups, being symmetry forbidden, could not be detected. The organo-gallium complexes, in general, exhibited three absorption maxima which are red shifted from the values for the corresponding free ligand. The low energy shoulder ~430 nm is arising due to the n–π* transitions. Appearance of this absorption in the complexes is indicative of less symmetric environment of the ligand moiety in the complexes. The red shift of the π–π* transitions in the complexes can be attributed to the increase in electron density in the ligand moiety brought about by the combined effect of the removal of proton present in the OH group of the salicylidene ligand accompanied by coordination with the gallium atom [3].

When a dichloromethane solution of **5c** was exposed to UV-radiation, there was a gradual change in the absorption spectrum with increase in the time duration of irradiation (Fig. 3). The initial absorption at 367 and 431(sh) nm are blue-(~344 nm) and red-

Table 1
Selected bond lengths (Å) and angles (°) for [$Me_2GaOC_6H_3$(N=NPh)CH=NPh]·½·C_6H_6 (**5a**·½·C_6H_6) and [$Me_2GaOC_6H_3$(N=NPh)CH=Ntol-4] (**5c**).

	(**5a**·½C_6H_6)	(**5c**)
Ga1–C20	1.950 (5)	1.927 (9)
Ga1–C21	1.949 (5)	1.965 (10)
Ga1–O1	1.908 (3)	1.865 (7)
Ga1–N1	2.029 (4)	2.037 (7)
C1–N1	1.286 (6)	1.273 (10)
N2–N3	1.248 (5)	1.247 (9)
C6–N2	1.414 (6)	1.420 (11)
C8–N3	1.427 (6)	1.408 (12)
C20–Ga1–C21	125.7 (2)	127.5 (5)
C20–Ga1–N1	108.1 (2)	105.0 (4)
C21–Ga1–N1	107.17 (19)	108.4 (4)
C20–Ga1–O1	109.8 (2)	110.8 (4)
C21–Ga1–O1	108.4 (2)	107.2 (4)
O1–Ga1–N1	92.50 (14)	92.1 (3)
C1–N1–Ga1	123.6 (3)	124.3 (7)
C14–N1–Ga1	117.0 (3)	116.1 (6)
C3–O1–Ga1	129.5 (3)	129.3 (6)
C6–N2–N3	114.5 (4)	115.2 (8)
N2–N3–C8	114.9 (4)	114.4 (8)
C1–N1–C14	119.4 (4)	119.5 (8)

(~436 nm) shifted and initial color change was also noted (yellow to yellow orange). Such blue and red shift in the absorption peak maxima have been reported on conversion of the *trans* isomer to *cis* form of azobenzene based systems [32]. On refluxing this solution (40 °C), color was faded slightly with the change in absorption maxima indicating the conversion of *cis* form to more stable *trans* form (Fig. 3) [32]. Similar changes in the absorption spectra of the free ligand were also observed (Supplementary information), However, these changes were rather small relative to the complexes.

Emission spectra of the ligands and their complexes were recorded in dichloromethane and the resulting data are summarized in Table 2. Emission spectra of ligands **1a**, **1b** and **4** are characterized by a broad peak centered at ~460 nm with a shoulder in the higher energy region (~400 nm) (Fig. 4). Corresponding excitation spectra (monitored at the emission maxima) also showed an asymmetric line shape with a shoulder towards higher energy values. The two peaks can be attributed to the $\pi-\pi^*$ transition taking place with the *trans* and *cis* forms of the ligand molecules respectively. The weak peak at the lower energy of the excitation peak originates from the forbidden $n \rightarrow \pi^*$ transition. The difference in the wavelength maximum corresponding to emission and excitation peaks (Stokes shift) for the ligands are in the range of 135–151 nm. Such a large value of Stokes shift indicates that the excited state of the ligands undergo significant changes with absorption of UV light. It is worth noting that many of the salicylidene aniline based ligands undergo intra-molecular proton transfer reaction in the excited state and is characterized by large Stokes Shift [33–35]. Higher values of the Stokes shift observed in the present study indeed confirm the occurrence of excited state intramolecular proton transfer (ESIPT) in these ligands. The electron donating substituents on the phenyl ring attached to the azomethine group in the ligands increase the electron density in the ligand and hence favors the excited state proton transfer reaction thereby stabilizing the keto group. This leads to marginal changes in the emission peak maxima. Once the ligand undergoes complexation with the metal, the excited state proton transfer phenomenon does not occur and this is reflected in the low values of Stokes shift observed from the complexes. A similar trend is also observed in our earlier studies [3] involving gallium complexes. Unlike the spectra of free ligands, the emission spectra from the complexes showed asymmetric peak centered ~400 nm and are blue shifted with respect to the free ligand. The blue-shift in the emission spectra is due to the absence of ESIPT in the gallium complexes [3]. Quantum yield values are always higher for the complexes compared to the ligands (Table 2). This could be due to reduced extent of non-radiative processes in the absence of ESIPT.

The ligands **2** and **3** and their complexes (**6a**, **6b**, **7a** and **7b**) are non-emissive in solution at room temperature. The emission from such ligands and their complexes appear to be significantly quenched by non-radiative processes occurring in the excited states (π^* or σ^*) of the molecules. These non-radiative processes normally depend on the nature of the existing inter- and intramolecular interactions in such molecules in a particular medium. Alternatively the non-rigidity of **2** and **3** and their complexes may be contributing to their non-emissive nature. An increase in rigidity often results in decrease in non-radiative decay leading to enhanced fluorescence.

Theoretical studies

The optimized structures of bare salicylaldimine Schiff base (**1b**) and its diorganogallium complex (**5c**) in *trans* and *cis* forms are depicted in Figs. 5 and 6, respectively. As has been shown experimentally above the *trans* form of free ligands as well as the complexes are more stable as compared to the corresponding *cis* form. This is also substantiated theoretically. The calculated metal ligand bond lengths (Table 3) are longer for the *cis* form than that for the

Table 2
UV–vis absorption, excitation and emission data of ligands and their organo gallium complexes in dichloromethane.

Compounds	UV–Vis absorption, λ in nm	Excitation λ in nm	Emission λ in nm	Stoke shift	Quantum yield (η) in %
[Ph–N=N–C_6H_3(4′–OH)–3′-CH=N–Ph] (**1a**)	274, 334	314	465	151	3
[Ph–N=N–C_6H_3(4′–OH)–3′-CH=N-tol-4)] (**1b**)	271, 336	318	460	142	3
[{Ph–N=N–C_6H_3(4′–OH)–3′-CH=N–CH_2}$_2$] (**2**)	285,361		–		
[{Ph–N=N–C_6H_3(4′–OH)–3′-CH=N–CH_2CH_2}$_3$N] (**3**)	275, 346		–		
[Ph–N=N–C_6H_3(4′–OH)–3′-CH=N–C_6H_4(OH-2″)] (**4**)	269, 337	321	456	135	2
[$Me_2GaOC_6H_3$(N=NPh) (CH=NPh)] (**5a**)	316, 364, 429(sh)	365	415	50	5
[$Et_2GaOC_6H_3$(N=NPh) (CH=NPh)] (**5b**)	317, 370, 435(sh)	356	407	51	5
[$Me_2GaOC_6H_3$(N=NPh) (CH=Ntol-4)](**5c**)	324, 366, 430(sh)	364	415	51	7
[$Et_2GaOC_6H_3$(N=NPh) (CH=Ntol-4)](**5d**)	322, 370, 431(sh)	357	403	46	3
[$Me_2GaOC_6H_3$(N=NPh) (CH=NCH_2–)]$_2$ (**6a**)	285, 361		–		
[$Et_2GaOC_6H_3$(N=NPh) (CH=NCH_2–)]$_2$ (**6b**)	274, 361		–		
[{$Me_2GaOC_6H_3$(N=NPh) (CH=NCH_2CH_2}$_3$N] (**7a**)	287, 363		–		
[{$Et_2GaOC_6H_3$(N=NPh) (CH=NCH_2CH_2}$_3$N] (**7b**)	282, 365		–		
[C_6H_5–N=N–C_6H_3(4′-OGaMeO)-3′-CH=N–C_6H_4] (**8a**)	314 (sh), 369, 438	357	406	49	8
[C_6H_5–N=N–C_6H_3(4′-OGaEtO)-3′-CH=N–C_6H_4] (**8b**)	316(sh), 370, 436	351	408	57	9

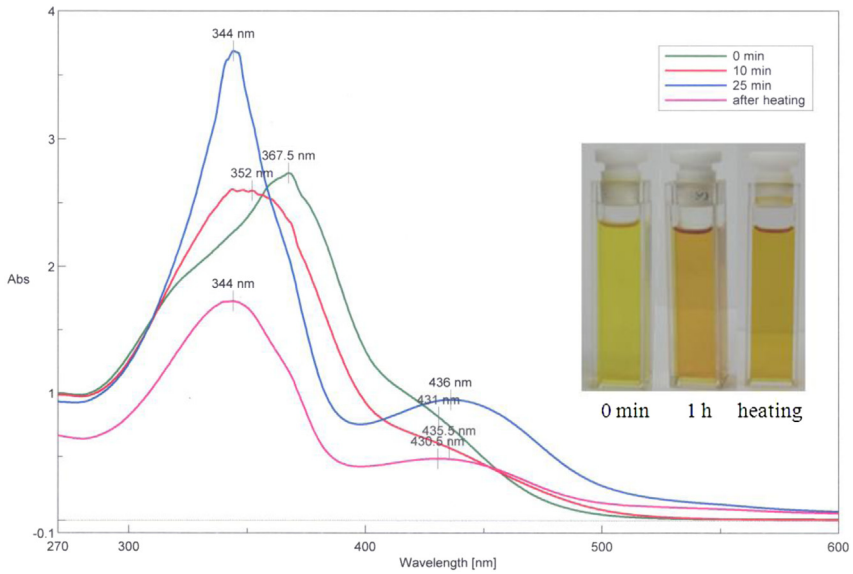

Fig. 3. UV absorption spectra of complex (**5c**) in dichloromethane on exposure UV radiation for different time periods followed by heating.

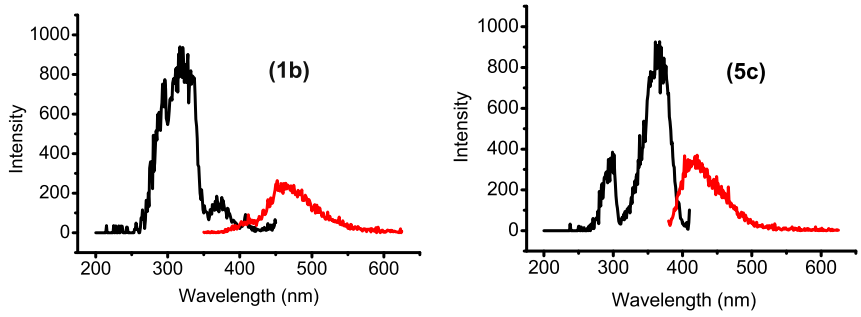

Fig. 4. Emission spectra for ligand (**1b**) and complex (**5c**) and the corresponding excitation spectra.

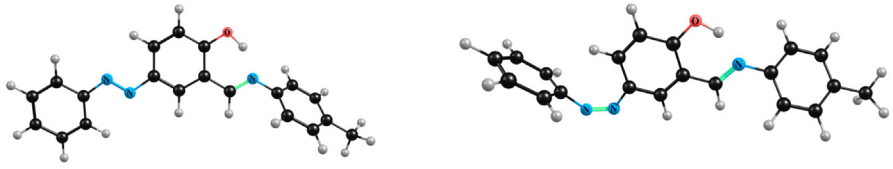

a) *trans* Isomer; total energy = -1012.19872149664 a. u b) *cis* Isomer; total energy = -1012.17338835368 a. u

Fig. 5. Optimized structure of bare [5-(phenylazo)-N-(p-toluidine)salicylidene] (**1b**) a) *trans* and b) cis isomers.

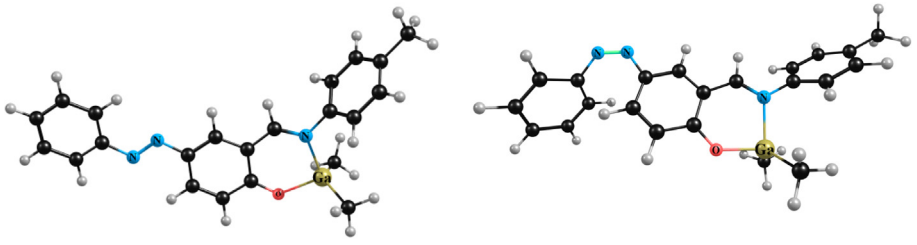

a) Ga-*trans* isomer;
total energy = -3016.64194929901 a. u.

b) Ga-*cis* isomer;
total energy = -3016.61730971694 a. u.

Fig. 6. Optimized structure of a) Ga-*trans* isomer and b) Ga-*cis* isomer of **5c**.

Table 3
Calculated M-L bond distances (Å) for Ga complexes using def-TZVP/BP86 method.

Complex	Ga–O	Ga–N	Ga–C
Ga-*trans* isomer	1.960	2.080	1.960
Ga-*cis* isomer	1.959	2.087	1.988

trans isomer. The calculated complexation energies (Table 4) also suggest that the *trans* isomer is more stable as compared to the *cis* isomer. Total energies for the free ligand and the complex also suggest that for both the cases, *trans* isomers are more stable. However, experimentally it has been found that on UV irradiation some amount of *trans* isomer is converted to the corresponding *cis* form and again on application of heat *cis* isomer reverts back to *trans* isomer for both bare ligands and complexes. This is due to a very small energy differences between the *cis* and *trans* isomers. We have also calculated the atomic charges on the metal and donor centers for the organo-gallium complexes with azo linked salicylaldimine Schiff bases. However there is not much difference in the atomic charge values (Table 5) on the metal and donor centers for both the isomers.

Conclusion

Mono- and di-organo gallium complexes derived from azo linked salicyladimine Schiff base have been synthesized. Mononuclear complexes are emissive in solution at room temperature. The emission peaks are blue-shifted with respect to the peak for the corresponding free ligand, but the Stokes shifts for the free ligands are always larger than that for the complexes. The quantum yields of the complexes are always higher than that for the corresponding ligands.

Experimental

Materials and physical measurements

All experiments involving organo-gallium compounds were carried out in anhydrous conditions under a nitrogen atmosphere using Schlenk techniques. Solvents were dried using standard methods. Triorganogallium etherates ($R_3Ga.OEt_2$; R = Me, Et) were prepared using gallium–magnesium alloy (Mg_5Ga_2) and alkyl iodide in diethyl ether. Ether contents in each preparation were evaluated by ^1H NMR integration [36]. The ligands, [5-(phenylazo)-N-(aniline)salicylidene] (**1a**), [5-(phenylazo)-N-(p-toluidine)salicylidene] (**1b**), bis(5-phenylazo salicyldehyde)ethylenediimine (**2**), tris{(5-phenylazo salicyldehyde)amino ethyl}amine (**3**) and [5-(phenylazo)-N-(2-hydroxyphenyl)salicylidene] (**4**), were prepared according to literature procedures [26,37,38] and were characterized by NMR spectroscopy (Supplementary material).

Infrared spectra were recorded as KBr plates on a Jasco FT-IR 6100 spectrometer. The NMR (^1H and $^{13}C\{^1H\}$) spectra were recorded on a Bruker Avance-II 300 spectrometer in 5 mm tubes as $CDCl_3$/dmso-d_6 solutions. Chemical shifts were referenced to internal chloroform/dimethyl sulfoxide peak. Electronic spectra were recorded in dichloromethane on a UV–vis Jasco V-630 spectrophotometer. All luminescence measurements were carried out at room temperature on an Edinburgh Instruments FLSP 920 system, having a 450 W Xe lamp. Quantum yields were measured using an integrating sphere coated with $BaSO_4$. All emission spectra were corrected for the detector response and excitation spectra for the lamp profile. Emission measurements were carried out with a resolution of 5 nm.

X-ray crystallography

Intensity data for $[Me_2GaOC_6H_3(N{=}NPh)CH{=}NPh]\cdot\frac{1}{2}C_6H_6$ (**5a**$\cdot\frac{1}{2}C_6H_6$) and $[Me_2GaOC_6H_3(N{=}NPh)(CH{=}Ntol\text{-}4)]$ (**5c**) were collected at room temperature on a Rigaku AFC 7S diffractometer using graphite monochromated Mo-Kα radiation (0.71069 Å). The structures were solved using direct methods [39] and refined by full matrix least square method [40] on F^2 using data corrected for absorption effects using empirical procedures [41]. All non-hydrogen atoms were refined anisotropically and hydrogen atoms were placed in their geometrically idealized positions with coordinate and thermal parameters riding on host atoms. The molecular structures are drawn using ORTEP [42]. Crystallographic and structural determination data are listed in Table 6.

Theoretical calculations

Theoretical calculations were carried out (for **1b** and **5c**) using density functional theory with Turbomole program package [43]. All the atoms have been treated at the all electron level and def-

Table 4
Calculated complexation energies (eV) for Ga complexes using def-TZVP/BP86 method.

Complex	Complexation energies (eV)
Ga-*trans* isomer	−49.12
Ga-*cis* isomer	−48.45

Table 5
Calculated atomic charges (Natural population analysis) on metal and donor centers of Ga complexes using def-TZVP/BP86 method.

Complex	q_{Ga}	q_O	q_N	q_C
Ga-*trans* isomer	1.590	−0.694	−0.535	−1.192
Ga-*cis* isomer	1.591	−0.694	−0.528	−1.194

Table 6
Crystallographic and structural refinement data for $[Me_2GaOC_6H_3(N{=}NPh)(CH{=}NPh)]\cdot\frac{1}{2}\cdot C_6H_6$ (**5a**$\cdot\frac{1}{2}\cdot C_6H_6$) and $[Me_2GaOC_6H_3(N{=}NPh)(CH{=}Ntol\text{-}4)]$ (**5c**).

Formula	$C_{21}H_{20}GaN_3O.\frac{1}{2}\cdot C_6H_6$ (**5a**$\cdot\frac{1}{2}C_6H_6$)	$C_{22}H_{22}GaN_3O$ (**5c**)
M	439.17	414.15
Size (mm)	0.20 × 0.15 × 0.05	0.25 × 0.20 × 0.10
Crystal system	Triclinic	Triclinic
Space group	P $\bar{1}$	P $\bar{1}$
a/Å	7.176 (2)	7.144 (5)
b/Å	13.198 (2)	12.300 (8)
c/Å	13.218 (3)	13.124 (8)
α/°	118.850 (12)	65.03 (5)
β/°	90.03 (3)	84.27 (5)
γ/°	99.63 (2)	77.35 (5)
V/Å^3	1076.2 (4)	1020.1 (11)
Z	2	2
d_{calc}/g cm^{-3}	1.355	1.348
μ (mm^{-1})/F(000)	1.297/454	1.364/428
θ for data collection/°	2.892–27.506	2.92–27.505
Limiting indices	$-5 \le h \le 9$ $-17 \le k \le 16$ $-17 \le l \le 17$	$-9 \le h \le 5$ $-15 \le k \le 15$ $-17 \le l \le 16$
No. of unique reflns	4947	4619
No. of obsd reflns with $I > 2\sigma(I)$	2612	1249
Data/restraints/parameters	4947/2/264	4619/0/247
Final R_1, ωR_2 indices (R_factor_gt/wR_factor_gt)	0.0638/0.1315	0.0778/0.1557
R_1, ωR_2 (all data) (R_factor_all/wR_Factor_ref)	0.1616/0.1520	0.3418/0.2430
Goodness of fit on F^2	0.989	0.904
Largest diff. peak and hole (e Å^{-3})	0.625 and −0.714	0.409 and −0.686

TZVP basis sets. The calculations have been performed with the generalized gradient approximation level of theory using Becke's exchange functional [44] in conjunction with Perdew's correlation functional (BP86) [45]. The metal-ligand bond lengths and complexation energy values have been calculated for the complexes. Charge distributions on the metal and donor centers have also been calculated using the natural population analysis scheme for the organo-gallium complexes with azo linked salicylaldimine Schiff bases.

Synthesis of complexes

*[$Me_2GaOC_6H_3$(N=NPh) (CH=NPh)] (**5a**)*

To a benzene solution (25 mL) of trimethylgallium etherate (274 mg, containing 100 mg (0.87 mmol) Me_3Ga), was added a solution of **1a** (262 mg, 0.87 mmol) with stirring which continued for 10 h. The solvent was evaporated under a reduced pressure to give an orange-red crystalline solid, which was recrystallized from hexane as an orange-red crystalline solid (254 mg, 73% yield), mp 133 °C, Anal. Calcd. for $C_{21}H_{20}GaNO_3$: C, 63.03; H, 5.04; N, 10.50%. Found: C, 62.99; H, 4.88; N, 10.27%. IR (υ in cm^{-1}): 1620 (C=N); 1474 (N=N); 590 (Ga–C); 530 (Ga–O). ^{1}H NMR (dmso-d_6) δ: −0.29 (s, Me_2Ga); 6.92 (d, $^3J_{HH}$ = 9.3 Hz, 1H); 7.44 -7.57 (m, 8H); 7.81(d, $^3J_{HH}$ = 7.8 Hz, 2H); 8.01(d, d, (2.4 Hz) $^3J_{HH}$ = 9.0 Hz, 1H); 8.27 (s, 1H); 8.91 (s, −CH=N−, 1H). ^{13}C{^{1}H} NMR (dmso-d_6) δ: −5.8 (s, Me_2Ga); 118.4 (C-1), 121.8, 122.1, 123.1, 128.1, 128.3, 129.4, 130.0, 130.5, 135.4, 142.8 (C-5), 146.3 (C-1″), 152.0 (C-1′), 169.2 (−CH=N−), 169.5 (C-2).

All the di-and mono-organo gallium complexes were prepared in a similar manner in 80–90% yield and were recyrstallized from toluene-hexane or dichloromethane-hexane mixture in 60–85 % yield.

*[$Et_2GaOC_6H_3$(N=NPh) (CH=NPh)] (**5b**)*

Prepared similar to **5a** and dissolved in hexane. The hexane soluble part was dried under reduced pressure to give a paste in 61% yield. IR (υ in cm^{-1}): 1614 (C=N); 1471 (N=N); 564 (Ga–C); 529 (Ga–O). ^{1}H NMR (dmso-d_6) δ: 0.38 (q, $^3J_{HH}$ = 7.8 Hz $-CH_2Ga$); 0.93 (t, $^3J_{HH}$ = 7.9 Hz CH_3CH_2Ga); 6.93 (d, $^3J_{HH}$ = 9.0 Hz, 1H); 7.44–7.59 (m, 8H), 7.80 (d, $^3J_{HH}$ = 7.5 Hz, 2H); 7.98 (d,d $^3J_{HH}$ = 2.4, 9.0 Hz, 1H); 8.25 (s, 1H), 8.98 (s, −CH=N−, 1H). ^{13}C{^{1}H} NMR (dmso-d_6) δ: 4.4 (s, $-CH_2Ga$); 10.0 (s, CH_3CH_2Ga); 118.9 (C-1), 122.0, 122.5, 123.4, 128.6, 129.0, 129.9, 130.5, 130.9, 135.9, 143.1, 146.9, 152.5, 170.0 (s, −CH=N−), 170.7 (C-2).

*[$Me_2GaOC_6H_3$(N=NPh) (CH=Ntol-4)] (**5c**)*

Prepared in 72% yield, mp 78 °C. Anal. Calcd for $C_{22}H_{22}GaN_3O$: C, 63.80; H, 5.35; N, 10.16%. Found: C, 63.17; H, 5.02; N, 10.25. %. IR (υ in cm^{-1}): 1617 (C=N); 1473 (N=N), 591(Ga–C); 536 (Ga–O). ^{1}H NMR (dmso-d_6) δ: −0.30 (s, Me_2Ga); 2.33 (s, $-CH_3$, 3H); 6.90 (d, $^3J_{HH}$ = 9.0 Hz, 1H); 7.32 (s, 4H); 7.47–7.56 (m, 3H); 7.80 (d, $^3J_{HH}$ = 7.2 Hz, 2H); 7.98(d, d, (1.2 Hz) $^3J_{HH}$ = 9.0 Hz, 1H); 8.23 (s, 1H); 8.86 (s, −CH=N−, 1H). ^{13}C{^{1}H} NMR (dmso-d_6) δ: −5.3 (s, Me_2Ga); 21.0 (Me), 118.9 (C-1), 122.0, 122.5, 123.4, 128.8, 129.8, 130.8, 130.9, 135.7, 138.2, 143.2, 144.2, 152.5, 168.8 (s, −CH=N−), 169.8(C-2).

*[$Et_2GaOC_6H_3$(N=NPh) (CH=Ntol-4)] (**5d**)*

Prepared in 63% yield as a paste. IR (υ in cm^{-1}): 1616 (C=N); 1468 (N=N); 562 (Ga–C); 535 (Ga–O). ^{1}H NMR (dmso-d_6) δ: 0.37 (q, $^3J_{HH}$ = 8.0 Hz $-CH_2Ga$); 0.93 (t, $^3J_{HH}$ = 8.0 Hz CH_3CH_2Ga); 2.36 (s, −Me); 6.92 (d, $^3J_{HH}$ = 9.3 Hz, 1H); 7.35 (s, 4H); 7.49–7.58 (m, 3H); 7.80 (d, $^3J_{HH}$ = 7.2 Hz, 2H); 7.98 (d,$^3J_{HH}$ = 2.4, 9.0 Hz, 1H); 8.23 (s, 1H), 8.96 (s, −CH=N−, 1H). ^{13}C{^{1}H} NMR (dmso-d_6) δ: 4.4 (s, $-CH_2Ga$); 10.0 (s, CH_3CH_2Ga); 21.0 (Me), 118.9 (C-1), 121.7, 122.5, 123.3, 128.9, 129.9, 130.9, 135.7, 138.3, 143.1, 144.5, 152.5, 169.2 (s, −CH=N−), 170.6 (C-2).

*[$Me_2GaOC_6H_3$(N=NPh) (CH=NCH_2−)]$_2$ (**6a**)*

Prepared similar to **5a** in 78% yield, mp 100 °C (decomp.). Anal. Calcd. for $C_{32}H_{34}Ga_2N_6O_2$: C, 57.12; H, 5.08; N, 12.46%. Found: C, 57.09; H, 5.21; N, 12.42%. IR (υ in cm^{-1}): 1627 (C=N); 1474 (N=N); 588 (Ga–C); 544, 533 (Ga–O). ^{1}H NMR (dmso-d_6) δ: −0.29 (s, Me_2Ga); 3.92 (s, $-CH_2-$, 4H); 6.86 (d, $^3J_{HH}$ = 8.4 Hz, 1H); 7.48–7.54 (m, 6H); 7.78 (d, $^3J_{HH}$ = 7.5 Hz, 4H); 7.94 (d, $^3J_{HH}$ = 8.1 Hz, 2H); 8.01 (s, 2H), 8.71 (s, −CH=N−, 2H). ^{13}C{^{1}H} NMR (dmso-d_6) δ: −6.2 (s, Me_2Ga); 57.0 ($-CH_2$), 117.8 (C-1), 122.1, 122.9, 1283, 129.4, 130.5, 133.3, 142.6, 152.0, 169.1(C-2), 172.7 (s, −CH=N−).

*[$Et_2GaOC_6H_3$(N=NPh) (CH=NCH_2−)]$_2$ (**6b**)*

Prepared similar to **6a** in 66% yield, mp 155 °C Calcd. for $C_{36}H_{42}Ga_2N_6O_2$: C, 59.21; H, 5.80; N, 11.52%. Found: C, 59.32; H, 5.73; N, 11.16%. IR (υ in cm^{-1}): 1621 (C=N); 1473 (N=N); 560 (Ga–C); 532 (Ga–O). ^{1}H NMR (dmso-d_6) δ: 0.41 (q, $^3J_{HH}$ = 7.9 Hz $-CH_2Ga$); 1.00 (t, $^3J_{HH}$ = 7.8 Hz CH_3CH_2Ga); 3.92 (s, $-CH_2-$, 4H); 6.89 (d, $^3J_{HH}$ = 9.0 Hz, 2H); 7.46–7.57 (m, 6H); 7.79 (d, $^3J_{HH}$ = 7.2 Hz, 4H); 7.96 (d, $^3J_{HH}$ = 9.3 Hz, 2H); 8.01 (s, 2H); 8.80 (s, −CH=N−, 2H). ^{13}C{^{1}H} NMR (dmso-d_6): 3.8 (s, $-CH_2Ga$); 10.0 (s, CH_3CH_2Ga); 56.4 (NCH_2), 118.3 (C-1), 122.5, 123.2, 128.8, 129.2, 129.8, 130.9, 133.8, 142.8, 152.5, 170.3 (C-2), 173.6 (s, −CH=N−).

*[{$Me_2GaOC_6H_3$(N=NPh) (CH=NCH_2CH_2}$_3$N] (**7a**)*

Prepared similar to **5a** in 84% yield, mp 89 °C. Anal. Calcd. for $C_{51}H_{57}Ga_3N_{10}O_3$: C, 57.39; H, 5.38; N, 13.12%. Found: C, 57.41; H, 5.24; N, 12.95%.IR (υ in cm^{-1}): 1628 (C=N); 1474 (N=N); 587(Ga–C); 532 (Ga–O). ^{1}H NMR (dmso-d_6) δ: −0.32 (s, Me_2Ga); 2.92 (t, $^3J_{HH}$ = 7.0 Hz, $-CH_2-$, 6H); 3.72 (t, $^3J_{HH}$ = 6.8 Hz, $-CH_2-$, 6H); 6.83(d, $^3J_{HH}$ = 9.0 Hz, 3H); 7.47–7.55 (m, 9H); 7.77 (d, $^3J_{HH}$ = 6.8 Hz, 6H); 7.91(d, $^3J_{HH}$ = 9.0 Hz, 3H); 8.00 (s, 3H); 8.64 (s, −CH=N−, 3H). ^{13}C{^{1}H} NMR (dmso-d_6) δ: −5.9 (s, Me_2Ga); 53.7 ($-CH_2-$), 54.7($-CH_2-$), 118.3 (C-1), 122.5, 123.2, 129.8, 130.9, 133.5, 143.0152.5, 169.4(C-2), 171.8 (s, −CH=N−).

*[{$Et_2GaOC_6H_3$(N=NPh) (CH=NCH_2CH_2}$_3$N] (**7b**)*

Prepared in 84% yield, mp 70 °C Calcd. for $C_{57}H_{69}Ga_3N_{10}O_3$: C, 59.46; H, 6.04; N, 12.16%. Found: C, 59.32; H, 5.73; N, 11.16%. IR (υ in cm^{-1}): 1626 (C=N); 1473 (N=N); 560 (Ga–C); 530 (Ga–O). ^{1}H NMR (dmso-d_6) δ: 0.37 (q, $^3J_{HH}$ = 7.4 Hz $-CH_2Ga$); 1.00 (t, $^3J_{HH}$ = 6.9 Hz CH_3CH_2Ga); 2.95 (s, $-CH_2-$, 6H); 3.71 (s, $-CH_2-$, 6H); 6.86 (d, $^3J_{HH}$ = 8.7 Hz, 3H); 7.50–7.53 (br, m, 9H); 7.76–7.79 (br, m 6H); 7.92 (d, $^3J_{HH}$ = 8.1 Hz, 3H); 8.01 (s, 3H); 8.71 (s, −CH=N−, 3H). ^{13}C{^{1}H} NMR (dmso-d_6): 3.7 (s, $-CH_2Ga$); 10.0 (s, CH_3CH_2Ga); 53.7 ($-CH_2-$), 54.8 ($-CH_2-$), 118.4 (C-1), 122.5, 123.1, 129.8, 130.8, 133.5, 142.9, 152.5, 170.2(C-2), 172.4 (s, −CH=N−).

*[C_6H_5–N=N–C_6H_3(4′-OGaMeO)-3′-CH=N–C_6H_4] (**8a**)*

Prepared similar to **5a** in 85% yield, mp 255 °C (decomp) Anal. Calcd. for $C_{20}H_{16}GaN_3O_2$: C, 60.04; H, 4.03; N, 10.50%. Found: C, 60.03; H, 4.31; N, 10.44, %. IR (υ in cm^{-1}): 1614 (C=N); 1483 (N=N), 576(Ga–C); 515 (Ga–O). ^{1}H NMR (dmso-d_6) δ: −0.53 (s, MeGa); 6.60 (t, $^3J_{HH}$ = 7.02 Hz, 1H); 6.70 (d, $^3J_{HH}$ = 7.8 Hz, 1H); 6.87(d, $^3J_{HH}$ = 9.0 Hz, 1H); 7.08 (t, $^3J_{HH}$ = 7.5 Hz, 1H); 7.48–7.57 (m, 3H); 7.62 (d, 7.80 $^3J_{HH}$ = 7.8 Hz, 1H); 7.80 (d, $^3J_{HH}$ = 7.5 Hz, 2H); 7.90 (d, $^3J_{HH}$ = 8.7 Hz, 1H); 8.13 (s, 1H); 9.11 (s, −CH=N−, 1H). ^{13}C{^{1}H} NMR (dmso-d_6) δ: −6.7 (s, MeGa); 115.7, 115.8, 117.8, 119.7 (C-1), 122.5, 123.5, 127.4, 129.8, 130.5, 130.7, 132.2, 132.3, 143.0, 152.6, 158.0 (s, −CH=N−), 159.2 (C-2″), 170.6 (C-2).

*[C_6H_5–N=N–C_6H_3(4′-OGaEtO)-3′-CH=N–C_6H_4] (**8b**)*

Prepared similar to **5a** and washed with hexane to give 86% yield, mp 265 °C (decomp.). Calcd. for $C_{21}H_{18}GaN_3O_2$: C, 60.91; H, 4.38; N, 10.14%. Found: C, 60.66; H, 4.25; N, 10.08%. IR (υ in cm^{-1}): 1615 (C=N); 1473 (N=N), 557 (Ga–C); 528 (Ga–O). ^{1}H NMR

(dmso-d_6) δ: 0.20 (q, $^3J_{HH}$ = 8.0 Hz $-CH_2Ga$); 0.81 (t, $^3J_{HH}$ = 8.1 Hz CH_3CH_2Ga); 6.60 (t, $^3J_{HH}$ = 7.5 Hz, 1H); 6.70 (d, $^3J_{HH}$ = 8.1 Hz, 1H); 6.87 (d, $^3J_{HH}$ = 9.0 Hz, 1H); 7.08 (t, $^3J_{HH}$ = 7.5 Hz, 1H); 7.49 (d, 3JHH = 6.7 Hz, 1H); 7.54 (t, 3JHH = 7.05 Hz, 2H); 7.63 (d, $^3J_{HH}$ = 7.5 Hz, 1H); 7.80 (d, $^3J_{HH}$ = 7.5 Hz, 2H); 7.90 (d,$^3J_{HH}$ = 2.4, 8.7 Hz, 1H); 8.11 (s, 1H); 9.14 (s, −CH═N−, 1H). $^{13}C\{^1H\}$ NMR in DMSO-d6: 4.7 (s, $-CH_2Ga$); 10.2 (s, CH_3CH_2Ga); 115.6, 115.8, 117.7, 120.0 (C-1), 122.4, 123.4, 127.5, 129.8, 130.5, 130.7, 131.9, 132.6, 143.0, 152.6, 158.0 (s, −CH═N−), 159.9(C-2″), 170.9(C-2).

Appendix A. Supplementary Data

CCDC-Nos. 1028336 and 1007737 contain the supplementary crystallographic data for $[Me_2GaOC_6H_3(N{=}NPh)CH{=}NPh]\cdot\frac{1}{2}C_6H_6$ (**5a**·$\frac{1}{2}C_6H_6$) and $[Me_2GaOC_6H_3(N{=}NPh)(CH{=}Ntol\text{-}4)]$ (**5c**) for this paper. These data can be obtained free of charge from The Cambridge Crystallographic Data Centre via www.ccdc.cam.ac.uk/data_request/cif.

Appendix B. Supplementary data

Supplementary data related to this article can be found at http://dx.doi.org/10.1016/j.jorganchem.2014.10.024.

References

[1] S. Schulz, in: C.E. Housecraft (Ed.), Comprehensive Organometallic Chemistry-III, vol 3, Elsevier, Oxford, 2007. Chapter 3.07.
[2] (a) N. Kushwah, M.K. Pal, A.P. Wadawale, V. Sudarsan, D. Manna, T.K. Ghanty, V.K. Jain, Organometallics 31 (2012) 3836;
(b) M.K. Pal, N. Kushwah, A.P. Wadawale, V.K. Jain, J. Chem. Res. (2010) 485.
[3] M.K. Pal, N. Kushwah, D. Manna, A.P. Wadawale, V. Sudarsan, T.K. Ghanty, V.K. Jain, Organometallics 32 (2013) 104.
[4] N.P. Kushwah, M.K. Pal, A.P. Wadawale, V.K. Jain, J. Organomet. Chem. 694 (2009) 2375.
[5] S. Araki, T. Hirashita, in: P. Knochel (Ed.), Comprehensive Organometallic Chemistry-III, vol. 9, Elsevier, Oxford, 2007. Chap 9.14.
[6] S. Ghoshal, A. Wadawale, V.K. Jain, M. Nethaji, J. Chem. Res. (2007) 221.
[7] L.G. Bloor, C.J. Carmalt, D. Pugh, Coord. Chem. Rev. 255 (2011) 1293.
[8] G. Bandoli, A. Dolmella, F. Tisato, M. Porchia, F. Refosco, Coord. Chem. Rev. 253 (2009) 56. A. R. Timerbaev, Metallomics, 1 (2009) 193.
[9] M.A. Jakupec, M. Galanski, V.B. Arion, C.G. Hartinger, B.K. Keppler, Dalton Trans. (2008) 183.
[10] C.W. Tang, S.A. van Slyke, Appl. Phys. Lett. 51 (1987) 913.
[11] C.H. Chen, J. Shi, Coord. Chem. Rev. 171 (1998) 161;
S. Wang, Coord. Chem. Rev. 215 (2001) 79.
[12] V.A. Montes, R. Pohal, J. Shinar, P.J. Anzenbacher, Chem. Eur. J. 12 (2006) 4523.
[13] P.E. Burrows, L.S. Sapochak, D.M. McCatty, S.R. Forrest, Appl. Phys. Lett. 64 (1994) 2718. Y. Wang, W. Zhang, Y. Li, L. Ye and G. Yang, Chem. Matter. 11 (1999) 530; L. S. Sapochak, A. Padmaperuma, N. Washton, F. Endrino, G. T. Schmett, J. Marshall, D. Fogarty, P. E. Burrows, and S. R. Forrest, J. Am. Chem. Soc., 123 (2001) 6300.
[14] A. Kagkepari, V. Bekiari, E. Stathatos, G.S. Papaefstathiou, C.P. Raptopoulou, T.F. Zafiropoulous, P. Lianos, J. Lumin. 129 (2009) 578.
[15] A. Kagkepari, G.S. Papaefstathiou, C.P. Raptopoulou, T.F. Zafiropoulos, Polyhedron 28 (2009) 3279.
[16] J. Qiao, L.D. Wang, L. Duan, Y. Li, D.Q. Zhang, Y. Qui, Inorg. Chem. 43 (2004) 5096.
[17] Y. Shen, H. Gu, Y. Zhu, Y. Pan, J. Organomet. Chem. 691 (2006) 1817.
[18] (a) R.W. Chestnut, R.R. Cesati III, C.S. Cutter, S.L. Pluttic, J.A. Kodzenelleubogen, Organometallics 17 (1998) 4889;
(b) J. Lewinski, J. Zachara, K.B. Starowieyski, Z. Ochal, I. Justyniak, T. Kopec, P. Stolarzewic, M. Dranka, Organometallics 22 (2003) 3773.
[19] A.D. Towns, Dyes Pigments 42 (1999) 3.
[20] H.G. Gray, R.A. Sharma, J. Med. Chem. 12 (1996) 1122.
[21] S.J. Isak, E.M. Eyring, J.D. Spikes, P.A. Meekins, J. Photochem. Photobiol. A 134 (2000) 77.
[22] M. Kurihara, H. Nishihara, Coord. Chem. Rev. 226 (2002) 125.
[23] H.M.D. Bandara, S.C. Burdette, Chem. Soc. Rev. 41 (2012) 1809.
[24] M. Odabasoglu, C. Albayrak, R. Ozkanca, F.Z. Aykan, P. Lonecke, J. Mol. Struct. 840 (2007) 71.
[25] J. Jayabharathi, V. Thanikachalam, M.V. Perumal, N. Srinivasan, Spectrochim. Acta A 83 (2011) 200.
[26] (a) A.A. Khandar, B. Shaabani, F. Belaj, A. Bakhtiari, Inorg. Chim. Acta 360 (2007) 3255;
(b) H. Dinçalp, F. Toker, İ. Durucasu, N. Avcıbaşı, S. Icli, Dyes Pigments 75 (2007) 11;
(c) P. Pattanayak, D. Patra, J.L. Pratihar, A. Burrows, M.F. Mahon, S. Chattopadhyay, Inorg. Chim. Acta 363 (2010) 2865;
(d) I.S. Ahmed, M.M. Moustafa, M.M.A. ElAziz, Spectrochim. Acta A 78 (2011) 1429;
(e) C. Anitha, C.D. Sheela, P. Tharmaraj, S. Sumathi, Spectrochim. Acta A 96 (2012) 493;
(f) A. Khandar, B. Shaabani, F. Belaj, A. Bakhtiari, Polyhedron 25 (2006) 1893.
[27] J. Weidlein, Z. Anorg. Allg. Chem. 386 (1971), 129.
[28] R.S. Tobias, M.J. Spragne, G.E. Glass, Inorg. Chem. 7 (1968) 1714.
[29] M.K. Pal, N.P. Kushwah, A.P. Wadawale, V.S. Sagoria, V.K. Jain, E.R.T. Tiekink, J. Organomet. Chem. 692 (2007) 4237.
[30] H.R. Hoveyda, S.J. Rettig, C. Orvig, Inorg. Chem. 32 (1993) 4909.
[31] L. Kalita, M.G. Walawalkar, R. Murugavel, Inorg. Chim. Acta 377 (2011) 105.
[32] M.E. Moustafa, M.S. McCready, R.J. Puddephatt, Organometallics 31 (2012) 6262.
[33] F. Hamon, F.D. Pilard, F. Barbot, C. Len, Tetrahedron 65 (2009) 10105.
[34] K. Ogawa, J. Harada, T. Fujiwara, S. Yoshida, J. Phys. Chem. A 105 (2001) 3425.
[35] M. Mukhopadhyay, D. Banerjee, A. Koll, A. Filarowski, S. Mukherjee, Spectrochim. Acta Part A 62 (2005) 126.
[36] K.B. Bhatt, S.M. Chopade, D. Dutta, V.K. Jain, N. Prasad, A.Y. Shah, BARC: R:001, 2002.
[37] A.A. Khandar, K. Nejati, Polyhedron 19 (2000) 607.
[38] A.K. Mahapatra, S.K. Manna, P. Saho, Talanta 85 (2011) 2673.
[39] A. Altomare, G. Cascarano, C. Giacovazzo, A. Guagliardi, J. Appl. Crystallogr. 27 (1994) 435.
[40] G.M. Sheldrick, Acta Crystallogr. A64 (2008) 112.
[41] T. Higashi, ABSCOR-Empirical Absorption Correction Based on Fourier Series Approximation, vol. 3, Rigaku Corporation, Matsubara, Akishima, Japan, 1995, pp. 9–12.
[42] L.J. Farrugia, J. Appl. Crystallogr. 30 (1997) 565.
[43] R. Ahlrichs, M. Bär, M. Häser, H. Horn, C. Kölmel, Chem. Phys. Lett. 162 (1988 : 1989) 165.
[44] A.D. Becke, Phys. Rev. A 38 (1988) 3098–3100.
[45] J.P. Perdew, Phys. Rev. B 33 (1986) 8822–8824.